

## Synthesis of Monofunctionalized Gold Nanoparticles by Fmoc Solid-Phase Reactions

Kie-Moon Sung,<sup>†</sup> David W. Mosley,<sup>†</sup> Beau R. Peelle,<sup>‡,§</sup> Shuguang Zhang,<sup>\*,‡</sup> and Joseph M. Jacobson<sup>\*,†</sup>

Center for Bits and Atoms, Center for Biomedical Engineering, and Department of Biology and Biological Engineering, Massachusetts Institute of Technology, 77 Massachusetts Avenue, Cambridge, Massachusetts 02139

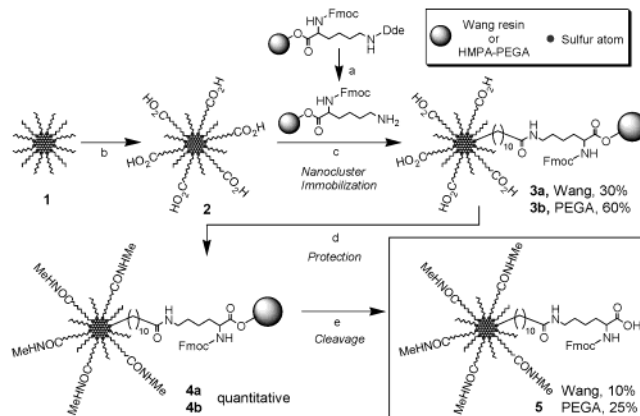
Received January 23, 2004; E-mail: jacobson@media.mit.edu

Recent progress in nanotechnology has shown highly promising capabilities of nanoparticles (NP) to function as powerful new biological sensory labels and electronic and optical devices.<sup>1</sup> Our laboratory demonstrated that a 1.4-nm gold NP covalently linked to an oligonucleotide is susceptible to radio frequency magnetic fields enabling remote electronic control over the reversible behavior of DNA hybridization.<sup>2</sup> For more elaborate biomolecular controls, multi-NP systems are of interest due to their expected synergistic or interfering ensemble properties with an enhanced complexity. Models for self-assembled hierarchies consisting of nano-building blocks have been suggested,<sup>3</sup> but manipulation with molecular level accuracy is required for precise and reliable fabrication of more complex structures comprising NP building blocks. The protective organic layer of capped NP provides sites for a variety of chemical modifications, yet to date precise control over functional ligand composition has been uncommon and extremely difficult to achieve because reactions heavily rely on unbalanced stoichiometries between small molecules and relatively massive NPs.

We report a versatile monofunctionalization method for gold NPs with L-lysine (Lys). These are potential building blocks for 1D NP peptide chains. Peptides are ubiquitous in biology and afford a wealth of 3D spatial structures and functions, and their exact properties are dictated by the linear order and composition of amino acids. Precise sequential positioning of NPs can be accomplished using peptide synthesis protocols. For this purpose, an amino acid NP building block should meet the following requirements: (a) single amino acid functionality per particle, (b) sufficiently small and uniform core diameters of  $\sim 2$  nm, a comparable size with major biomolecules, (c) amphiphilic solubility in aqueous and organic media enabling manual or programmed peptide synthesis, and (d) ease of synthesis with minimized effort for purification. Several groups have attempted to string up NPs using rigid polymeric backbones or self-assembly strategies, but generally these methods have been unable to design complex or reliable nanostructures.<sup>4</sup>

To ensure monofunctionalization of NPs, which presents a gigantic challenge in chemical synthesis, we performed a solid-phase reaction. We took advantage of the low-density packing of functional groups present in many solid-phase supports. For example, each functional group on a common PS Wang resin bead possesses a rough volume of at least  $\sim 9$  nm<sup>3</sup> when suspended in DMF, and thus we hypothesized an NP  $\leq 2$  nm can be loaded on the solid phase through a single bond per particle.<sup>5</sup> As shown in Scheme 1, octanethiolate (CH<sub>3</sub>(CH<sub>2</sub>)<sub>7</sub>S<sup>-</sup>, OT) monolayer-protected gold NPs **1** were taken as robust precursor NPs.<sup>6</sup> Surface modification of **1** by ligand exchange with an excess 11-mercaptoundecanoic acid (HO<sub>2</sub>C(CH<sub>2</sub>)<sub>10</sub>SH, MUA) in THF afforded reactive amphiphilic NPs **2** in which both ligands are present in approximately equal amounts as reported in the literature.<sup>7</sup>

**Scheme 1.** Synthesis of Lys-Monofunctionalized Gold Nanoparticles<sup>a</sup>



<sup>a</sup> Reagents and conditions: (a) H<sub>2</sub>NNH<sub>2</sub>·H<sub>2</sub>O/DMF (2% v/v), DIPEA/DMF (10% v/v). (b) HS(CH<sub>2</sub>)<sub>10</sub>CO<sub>2</sub>H (excess), THF. (c) DIC (excess), DMF/THF (10% v/v) room temperature, 24 h. (d) MeNH<sub>2</sub>, DIC (excess), DMF/THF, room temperature, 12 h. (e) 60% TFA, 2.5% TIS, 2.5% H<sub>2</sub>O, 35% DMF, 24 h.

Core sizes of the NPs **1** and **2** were identified by high-resolution transmission microscopy (HRTEM), and their particle diameters were found to be  $2.0 \pm 0.3$  and  $2.1 \pm 0.2$  nm, respectively. Direct one-pot synthesis of MUA-protected gold NPs was attempted by modifying the method of Ulman and co-workers<sup>8</sup> but was not successful in obtaining monodisperse NPs.

A conventional solid-phase reaction using a 9-fluorenylmethoxycarbonyl (Fmoc) protecting group was then carried out for coupling of NP **2** with Lys. NPs **2** were treated with commercially available Fmoc-Lys(Dde)-Wang PS beads (Dde = 1-(4,4-dimethyl-2,6-dioxocyclohexylidene)ethyl), after the  $\epsilon$ -amine was deprotected, in the presence of 1,3-diisopropylcarbodiimide (DIC) under the conditions described in Scheme 1. On the basis of the weight gain of the beads, **2** was found to be consumed with  $\sim 30\%$  loading level to afford **3a**. High-temperature reaction at 80–100 °C improved NP loading up to  $\sim 50\%$ , but the solution color changed to burgundy red within 4 h with the plasmon resonance band at  $\lambda_{\text{max}} = 520$  nm, indicating a significant growth of larger particles of NPs. Features of elemental composition and morphology of **3a** were investigated by scanning electron microscopy (SEM)-assisted energy-dispersive X-ray analysis (EDX) (Supporting Information). A spot profile of nanoparticles immobilized on a resin exhibited the presence of strong signals from carbon and gold atoms, which are the characteristic elemental components of **3a**. To confirm a successful covalent coupling, a resin salt [(Fmoc-Lys-Wang)<sup>n+</sup>·**2**<sup>n-</sup>] was examined by SEM (Supporting Information). In this case, the ionic species cause charging effects, resulting in poorly resolved images, which is quite different from **3**.

Protection of the free carboxyl groups in **3a** was accomplished by a coupling reaction with a slight excess of methylamine to afford

<sup>†</sup> Center for Bits and Atoms.

<sup>‡</sup> Center for Biomedical Engineering.

<sup>§</sup> Department of Biology and Biological Engineering.

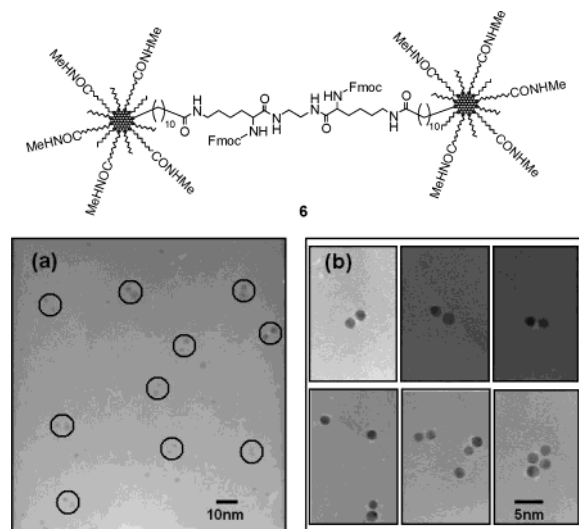


**Figure 1.** Schematic structure and HRTEM images of gold nanoparticle dimers **6**.

**4a** in an almost quantitative yield (Scheme 1). Subsequent Lys transfer from Wang resin to the gold nanoparticle was completed by treatment of the bead loaded with **4a** with an acidic cleavage cocktail, 60% trifluoroacetic acid (TFA) in DMF. The cleavage reaction typically took place in 2 h. The first crop of isolated nanoparticles **5** was obtained with  $\sim 10\%$  yield from **4a** and with  $\sim 3\%$  in overall from **2**.

Due to the low yield of the final product **5** from the reaction with PS Wang resin, we employed an alternative solid support, poly(ethylene glycol)acrylamide copolymer (PEGA)-based resin, which is widely used for on-bead enzyme assays.<sup>9</sup> Resin swelling is key to enhancing substrate permeability to increase loading levels, and PEGA was chosen because it swells approximately four times greater than PS resin in DMF. Fmoc-Lys(Dde)-OH was introduced to PEGA following the dichlorobenzoyl chloride (DBC) method with the use of a tethered linker, 4-hydroxymethylphenoxyacetyl (HMPA). Lys group substitution level on HMPA-PEGA resin was measured to be 0.05 mmol/g in DMF. The remaining procedures for the monofunctionalized gold NPs **5** were similar to those used for the PS Wang resin. Using PEGA beads, we could increase the NP loading level in **3b** and the yield of **5** from **4b** up to 60% and 25%, respectively. Therefore, an HMPA-PEGA support could achieve an overall 15% yield for **5** that is five times higher than that of PS Wang-supported synthesis.

The particle size of **5** remained similar to that of the precursors and was determined to be  $2.2 \pm 0.3$  nm by TEM. An FTIR measurement clearly distinguished **5** from **2** as evidenced by the strong amide I and II peaks at  $1700$  and  $1650$   $\text{cm}^{-1}$  and  $\nu(\text{N-H})$  at  $3270$   $\text{cm}^{-1}$  in **5**, respectively (Supporting Information). However, we have been unable to directly detect Lys on NP **5**, because its concentration is very low relative to the majority of the ligands in **5**.

Direct evidence of monofunctionalization is revealed by dimerization of the isolated NPs **5**, which were treated by a slow addition of bridging linker ethylenediamine (excess) in the presence of DIC. Since the carboxyl group of Lys in **5** is the only reactive moiety for reaction, it is possible to count the number of Lys present in **5** by identifying the associated NPs. As anticipated, TEM images in Figure 1a demonstrate that the dimeric species **6** are dominant and that 55–60% of particles on the TEM grid are found to undergo dimerization, reflecting that at least 55% NPs are monofunctionalized. The interparticle distance is  $1.8 \pm 0.5$  nm, which is less than the estimated 4.8-nm length for a fully extended bridge. This could indicate that the bridging ligand is coiled to the side and that

the ligand sphere of the particles may be interdigitated. Interestingly, there appears to be no significant difference in the dimerization features originating from the use of different solid supports. NPs **5** from either PS Wang resin or PEGA gave almost identical particle size distribution and dimerization efficacy of  $\sim 60\%$  toward **6**. Some monomers and higher-order clusters were observed (Figure 1b), suggesting that some particles may be functionalized by multiple Lys or may not have reacted in the dimerization reaction. It is uncertain whether these monomers and higher-order clusters contain significant amounts of monofunctionalized NPs, and the actual yield for monofunctionalized ones may be higher if a more accurate assay is found. This is a highly selective method for monofunctionalization of NPs compared to the routine stoichiometric reactions. For instance, Feldheim and co-workers have reported a stoichiometric assembly of gold NPs into dimers using a rigid bridging linker, and their efficiency in dimer formation was as high as  $\sim 47\%$ .<sup>10</sup>

In summary, we have synthesized  $\sim 2$ -nm sized Lys-monofunctionalized gold NPs **5** in a highly selective manner by solid-phase reaction using PS Wang resin or HMPA-PEGA. Productivity and reaction efficiency are highly dependent on the swelling properties of the solid support, which is not common in solid-phase organic synthesis. We are currently working to employ these NP building blocks in a peptide synthesis strategy.

**Acknowledgment.** This work was supported by grants from DARPA Biocomputing, DARPA/AFO NURI/AFO, and Things That Think Consortium of MIT Media Lab. We thank Michael Frongello and Vikas Anant for the electron microscopy measurements.

**Supporting Information Available:** Experimental details for the synthesis of the gold nanoparticles (PDF). This material is available free of charge via the Internet at <http://pubs.acs.org>.

## References

- (1) (a) Bruchez, M., Jr.; Moronne, M.; Gin, P.; Weiss, S.; Alivisatos, A. P. *Science* **1998**, *281*, 2013–2016. (b) Xiao, Y.; Patolsky, F.; Katz, E.; Hainfeld, J. F.; Willner, I. *Science* **2003**, *299*, 1877–1881. (c) Storhoff, J. J.; Mirkin, C. A. *Chem. Rev.* **1999**, *99*, 1849–1862 and references therein. (d) Thanh, N. T. K.; Rosenzweig, Z. *Anal. Chem.* **2002**, *74*, 1624–1628. (e) Maxwell, D. J.; Taylor, J. R.; Nie, S. *J. Am. Chem. Soc.* **2002**, *124*, 9606–9612. (f) Klein, D. L.; Roth, R.; Lim, A. K. L.; Alivisatos, A. P.; McEuen, P. L. *Nature* **1997**, *389*, 699–701. (g) Otsuka, H.; Akiyama, Y.; Nagasaki, Y.; Kataoka, K. *J. Am. Chem. Soc.* **2001**, *123*, 8226–8230.
- (2) Hamad-Schifferli, K.; Schwartz, J. J.; Santos, A. T.; Zhang, S.; Jacobson, J. M. *Nature* **2002**, *415*, 152–155.
- (3) Zhang, Z.; Horsch, M.; Lamm, M. H.; Glotzer, S. C. *Nano Lett.* **2003**, *3*, 1341–1346.
- (4) (a) Fullam, S.; Cottell, D.; Rensmo, H.; Fitzmaurice, D. *Adv. Mater.* **2000**, *12*, 1430–1432. (b) Stevenson, K. A.; Muralidharan, G.; Maya, L.; Wells, J. C.; Barhen, J.; Thundat, T. *J. Nanosci. Nanotechnol.* **2002**, *2*, 397–404. (c) Jiang, K.; Eitan, A.; Schadler, L. S.; Ajayan, P. M.; Siegel, R. W.; Grobert, N.; Mayne, M.; Reyes-Reyes, M.; Terrones, H.; Terrones, M. *Nano Lett.* **2003**, *3*, 275–277. (d) Marinakos, S. M.; Brousseau, L. C., III; Jones, A.; Feldheim, D. L. *Chem. Mater.* **1998**, *10*, 1214–1219. (e) Liao, J. H.; Chen, K. J.; Xu, L. N.; Ge, C. W.; Wang, J.; Huang, L.; Gu, N. *Appl. Phys. A* **2003**, *76*, 541–543. (f) Liao, J.; Zhang, Y.; Xu, L.; Ge, C.; Liu, J.; Gu, N. *Colloids Surf., A* **2003**, *223*, 177–183.
- (5) Values were estimated by calculation based on data for the functional group substitution level and resin swelling volume (1% DVB-cross-linked, 100–200 mesh, 0.54 mmol/g substitution level, swelling volume 3 mL/g in DMF), and solid matrix volume and porosity were not taken into account.
- (6) Hostetler, M. J.; Wingate, J. E.; Zhong, C.-J.; Harris, J. E.; Vachet, R. W.; Clark, M. R.; Londono, J. D.; Green, S. J.; Stokes, J. J.; Wignall, G. D.; Glish, G. L.; Porter, M. D.; Evans, N. D.; Murray, R. W. *Langmuir* **1998**, *14*, 17–30.
- (7) Simard, J.; Briggs, C.; Boal, A. K.; Rotello, V. M. *Chem. Commun.* **2000**, 1943–1944.
- (8) Yee, C. K.; Jordan, R.; Ulman, A.; White, H.; King, A.; Rafailovich, M.; Sokolov, J. *Langmuir* **1999**, *15*, 3486–3491.
- (9) Meldal, M. *Biopolymers* **2002**, *66*, 93–100.
- (10) (a) Novak, J. P.; Brousseau, L. C., III; Vance, F. W.; Johnson, R. C.; Lemon, B. I.; Hupp, J. T.; Feldheim, D. L. *J. Am. Chem. Soc.* **2000**, *122*, 12029–12030. (b) Novak, J. P.; Feldheim, D. L. *J. Am. Chem. Soc.* **2000**, *122*, 3979–1980. (c) Brousseau, L. C., III; Novak, J. P.; Marinakos, S. M.; Feldheim, D. L. *Adv. Mater.* **1999**, *11*, 447–449.

JA049578P